

# Magnetic Field Effect on Photoinduced Electron Transfer between Dibenzo[a,c]phenazine and Different Amines in Acetonitrile–Water Mixture

Debarati Dey,<sup>†</sup> Adity Bose,<sup>†</sup> Manas Chakraborty,<sup>‡</sup> and Samita Basu<sup>\*,†</sup>

Chemical Sciences Division, Saha Institute of Nuclear Physics, 1/AF, Bidhannagar, Kolkata 700 064, India, and Department of Chemistry, Bose Institute, 93/1, A.P.C. Road, Kolkata 700 009, India

Received: September 21, 2006; In Final Form: December 7, 2006

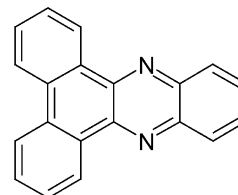
Unlike the simple phenazine (PZ) molecule, one of its derivatives, dibenzo[a,c]phenazine (DBPZ) forms a charge-transfer complex in the triplet state (<sup>3</sup>ECT) with different amines, e.g., N,N-dimethylaniline (DMA), 4,4'-bis(dimethylamino)diphenylmethane (DMDPM), and triethylamine (TEA). Formation of the <sup>3</sup>ECT and radical ion pairs (RIPs) due to electron transfer is identified by laser flash photolysis. The RIPs are much more abundant in the cases of DMA and DMDPM rather than in TEA. Interestingly, a prominent magnetic field effect (MFE) is observed in both the cases of <sup>3</sup>ECT and RIPs in homogeneous acetonitrile–water (MeCN/H<sub>2</sub>O) mixtures. This rare observation of the <sup>3</sup>ECT and MFE in non-viscous medium could be explained by considering the extended planar structure of DBPZ and inter-radical hydrogen bonding, mediated by the intervening water molecules. The magnetic field behavior is consistent with the hyperfine mechanism; however, the low  $B_{1/2}$  value for DBPZ–TEA system is ascribed to fast electron exchange due to the close proximity of the corresponding radical ions.

## Introduction

Electron-transfer reactions occur in a variety of chemical and biological processes.<sup>1</sup> In photoinduced electron transfer (PET) reactions, it essentially requires, for elucidation of the reaction mechanism, identifying the transient intermediates and recognizing the spin states where the initial electron transfer takes place. The radical ion pairs (RIPs), formed during PET as transient intermediates contain free electrons and are susceptible to magnetic field (MF).<sup>2–8</sup> The magnetic field effect (MFE) involves diffusive separation, singlet–triplet spin conversion, and geminate recombination or free ion formation of the partners of the geminate RIPs into the bulk solvent. The partners of the geminate RIPs undergo a diffusive separation to an optimum distance where the exchange interactions become negligible and intersystem crossing (ISC) occurs between the singlet and triplet RIPs. Application of an external MF, of the order of the hyperfine interactions (HFI) present in the system or higher, lifts the degeneracy, generally ascribed to Zeeman splitting, between the singlet and the triplet states and inhibits the ISC. This results in an increase of the population of the initial spin states of the RIPs. Therefore, MFE serves importantly to identify the initial electronic spin state of the RIPs.

Recently we have studied PET reactions between small drug-like molecules and different organic and DNA bases using a transient absorption technique, namely, laser flash photolysis and MFE.<sup>9,10</sup> Phenazine (PZ) derivatives represent one of the important classes of anticancer drugs.<sup>11</sup> We have synthesized a phenazine (PZ) derivative, dibenzo[a,c]phenazine (DBPZ), which, unlike the simple PZ molecule, has an extended planarity. In this paper we report a comparative study of PET reactions between dibenzo[a,c]phenazine (DBPZ) and some organic

## CHART 1



amines, namely, N,N-dimethylaniline (DMA), 4,4'-bis(dimethylamino)diphenylmethane (DMDPM), and triethylamine (TEA) in homogeneous acetonitrile (MeCN) and acetonitrile–water (MeCN/H<sub>2</sub>O) mixtures at room temperature. We could detect a charge-transfer complex of the DBPZ and the amines. We have found distinct MFE on the RIPs and the charge-transfer complex in homogeneous MeCN medium only in the presence of small amount of water molecules, which was not observed earlier with simple PZ molecule.<sup>9</sup> Generally MFE experiments on the triplet born transients using laser flash photolysis technique involve micellar media<sup>6,12,13</sup> or highly viscous solvents<sup>14–16</sup> at low-temperature or long-chain biradicals<sup>17,18</sup> to reduce fast escape, thus retaining the spin-correlation between the partners of the geminate RIPs. However, a few examples exist in the literature, where MFE has been detected in homogeneous medium by transient absorption of the triplets and the radical ions.<sup>19–27</sup> In our case, however, the extended planar structure of DBPZ as compared to that of PZ might be responsible for this observation.

## Experimental Section

DBPZ (Chart 1) was synthesized in the laboratory using the method mentioned in reference 28. It was purified by repeated crystallization with the purity checked by thin-layer chromatography (TLC), melting point, and mass spectroscopy. DM-

\* To whom correspondence should be addressed. E-mail address: samita.basu@saha.ac.in.

<sup>†</sup> Saha Institute of Nuclear Physics.

<sup>‡</sup> Bose Institute.

**TABLE 1:** Table for Absorption Data of Different Compounds in MeCN in Their Ground State

system	$\lambda_{\max}$ (nm)	system	$\lambda_{\max}$ (nm)
DBPZ	372, 392	$^3\text{DBPZ}^-$	560
DMA	302	$\text{DMA}^{+\cdot}$	450
DMDPM	264	$\text{DMDPM}^{+\cdot}$	460-480
TEA	$\sim 200$	$^3(\text{DBPZ}-\text{TEA complex})$	420

DPM was obtained from Aldrich and recrystallized from ethanol. DMA and TEA were obtained from SRL, India, and used after proper distillation. UV spectroscopy-grade MeCN and cyclohexane (CH) were obtained from Spectrochem and used as such without purification. Water was triply distilled.

Absorption data were taken using a Shimadzu UV-2101-PC absorption spectrophotometer. The transient absorption spectra were measured by using a nanosecond flash photolysis setup (Applied Photophysics) having an Nd:YAG laser (DCR-11, Spectra Physics) described elsewhere.<sup>29</sup> The sample was excited by 355 nm laser light with  $\sim 8$  ns FWHM. Transients were monitored through absorption of light from a pulsed Xe lamp (250 W). The photomultiplier (IP28) output was fed into a Tektronix oscilloscope (TDS 3054B, 500 MHz, 5Gs/s), and the data were transferred to a computer using the TekVISA software. MFE on the transient absorption spectra was studied by passing dc through a pair of electromagnetic coils placed inside the sample chamber. The strength of MF can be varied from 0.0 to 0.08 T. The software Origin 5.0 was used for curve fitting. The solid curves are obtained by connecting the points by using B-Spline option. All the samples were deaerated by passing pure argon gas for 20 min prior to the experiment. No degradation of the samples was observed during the experiment.

## Results and Discussion

Table 1 collects the absorption data for all the compounds and their corresponding transients. In MeCN the triplet-triplet absorption spectrum of DBPZ has a peak at 400 nm and a hump around 500 nm (Figure 1). Both the triplet peaks are quenched on addition of bases DMA, DMDPM, and TEA. However, different bases have different quenching characteristics as discussed in the following.

**Quenching Study with DMA and DMDPM.** In both the cases of DMA and DMDPM the quenching of the triplet DBPZ ( $^3\text{DBPZ}$ ) is accompanied by simultaneous appearance of new peaks at 420 and 560 nm. Other characteristic peaks also appear around 460 and 460–480 nm (broad) for the radical cations,  $\text{DMA}^{+\cdot}$  and  $\text{DMDPM}^{+\cdot}$ , respectively (Figures 1 and 2). These observations are quite similar to those with simple PZ. The appearance of the radical cations in each case is due to an electron transfer from DMA/DMDPM to DBPZ. The radical anion corresponding DBPZ is observed around 560 nm. Ogata et al. previously reported that the radical anion of PZ undergoes an absorption around 550 nm.<sup>32</sup> The transient absorption spectra of DBPZ with different concentration of DMA and DMDPM in Figures 1 and 2 show that the characteristic peak of  $^3\text{DBPZ}$  around 400 nm decreases gradually while that around 560 nm due to  $\text{DBPZ}^-$  and the respective cations of the bases increase simultaneously with the increasing concentration of bases. Clear isosbestic points have also been observed for both the bases, which are shown by circles in Figures 1 and 2. We have calculated the triplet state quenching constant for DBPZ at 400 nm with DMA and DMDPM from the slope of the Stern–Volmer relation

$$\tau^{-1} = \tau_0^{-1} + {}^1k_q[\text{Q}]$$

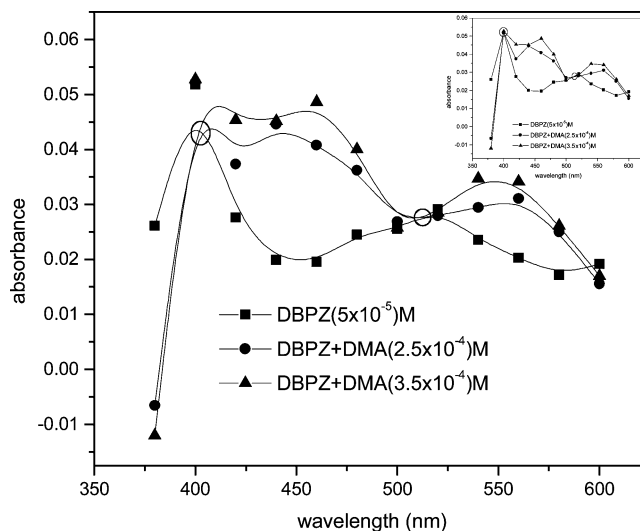


**Figure 1.** Transient absorption spectra of DBPZ ( $5 \times 10^{-5}$  M) at different DMA concentrations 0.0 (■),  $2.5 \times 10^{-4}$  (●), and  $3.5 \times 10^{-4}$  M (▲) in MeCN at  $0.6 \mu\text{s}$  after the laser flash (fitted with B-spline option). Inset shows the same spectra where experimental data points are directly joined. The isosbestic points are shown by ○.

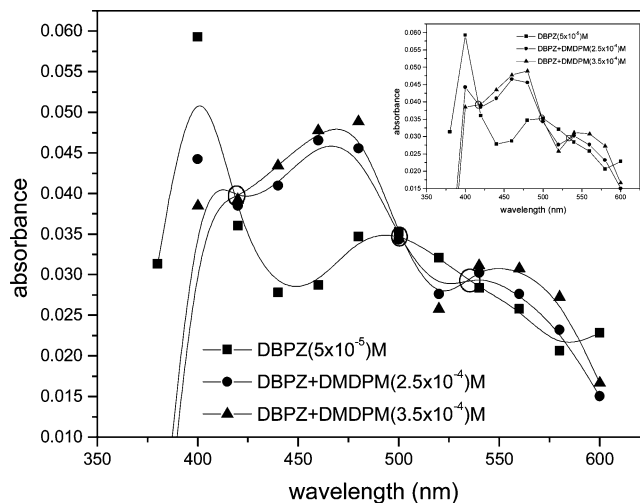


**Figure 2.** Transient absorption spectra of DBPZ ( $5 \times 10^{-5}$  M) at different DMDPM concentrations 0.0 (■),  $2.5 \times 10^{-4}$  (●), and  $3.5 \times 10^{-4}$  M (▲) in MeCN at  $0.6 \mu\text{s}$  after the laser flash (fitted with B-spline option). Inset shows the same spectra where experimental data points are directly joined. The isosbestic points are shown by ○.

where  $\tau_0^{-1}$  and  $\tau^{-1}$  are the reciprocal of the triplet lifetimes in absence and presence of the quencher (Q) and  ${}^1k_q$  is the triplet quenching constant, respectively. The quenching rate constants of the triplet states have been found to be  $1.27 \times 10^9$  and  $9.19 \times 10^8 \text{ M}^{-1} \text{ s}^{-1}$ , respectively, when DMA and DMDPM were used as quencher. From the values it could be assumed that the reactions are diffusion controlled, thus ruling out the possibility of energy transfer. The electron transfer, which is a diffusion-controlled phenomenon, might be responsible for the triplet quenching in both the cases. It has been already mentioned that another peak, absent in case of simple PZ molecule, shows up at 420 nm on addition of bases.<sup>31</sup> This is due to the formation of a new species, as its lifetime around 420 nm is somewhat longer compared to  $^3\text{DBPZ}$  or radical cation/anion. It is evident from Figures 1 and 2 that the formation of the species at 420 nm increases with increasing concentration of the bases. The increase in absorption intensity at 420 nm is more prominent in the case of DMA than that in DMDPM. This species at 420 nm is tentatively assigned to an excited-state charge-transfer

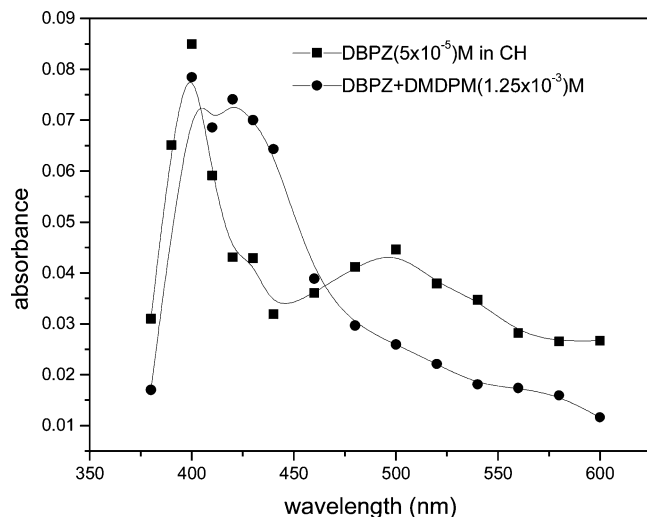
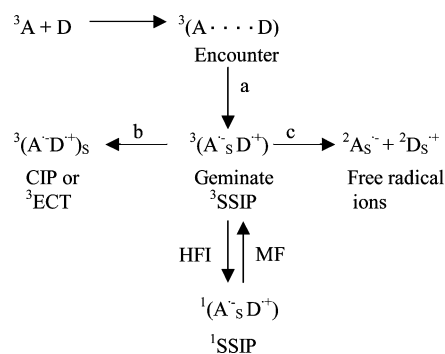


**Figure 3.** Transient absorption spectra of DBPZ ( $5 \times 10^{-5}$  M) (■) and DBPZ ( $5 \times 10^{-5}$  M)–DMDPM ( $1.25 \times 10^{-3}$  M) (●) at  $0.6 \mu\text{s}$  after the laser flash in cyclohexane.

### SCHEME 1



complex, which is much more prominent in a nonpolar solvent. A similar study with DBPZ and DMDPM in CH, instead of MeCN, shows a different type of quenching curves (Figure 3). In nonpolar solvent the radical cations and anions are not stabilized by solvation. Therefore, after the electron transfer from DMA/DMDPM to DBPZ, the corresponding ion formations are suppressed (path c, Scheme 1), while the charge-transfer complex formation is favored well (path b).

**Quenching Study with TEA.** When an aliphatic amine TEA instead of aromatic amines DMA/DMDPM is used as an electron donor, the triplet–triplet absorption of DBPZ is quenched with the rate constant of  $1.33 \times 10^9 \text{ M}^{-1} \text{ s}^{-1}$  at 400 nm. In this case neither the characteristic TEA radical cation at 380 nm<sup>9</sup> nor the DBPZ radical anion at 560 nm is observed, though the peak at 420 nm is quite prominent (Figure 4). However, with PZ in MeCN, only a systematic quenching of the triplet–triplet absorption is observed without the appearance of any new peak. The new transient species at 420 nm has a much longer lifetime ( $4.66 \mu\text{s}$ ) compared to that of  ${}^3\text{DBPZ}$  ( $2.69 \mu\text{s}$ ); the decay profiles are shown in the inset of Figure 5. This figure also shows the transient absorption spectra observed for DBPZ and TEA in MeCN at different times after the laser flash. The spectra clearly show that the triplet–triplet absorption of DBPZ decreases with time while the species at 420 nm increases from a time delay of 20 ns to that of 200 ns. This indicates that the triplet state is a precursor of the excited-state charge-transfer complex. So unlike the aromatic bases, the aliphatic base TEA restricts the electron transfer and facilitates the formation of an excited-state charge-transfer complex.

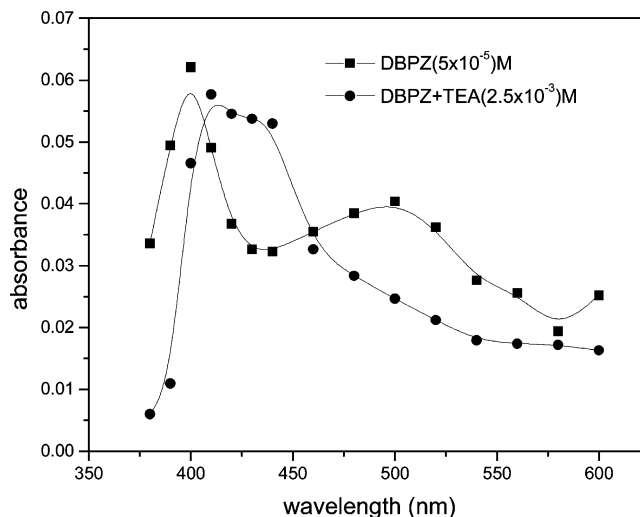


**Figure 4.** Transient absorption spectra of DBPZ ( $5 \times 10^{-5}$  M) (■) and DBPZ ( $5 \times 10^{-5}$  M)–TEA ( $2.5 \times 10^{-3}$  M) (●) at  $0.6 \mu\text{s}$  after the laser flash in MeCN.

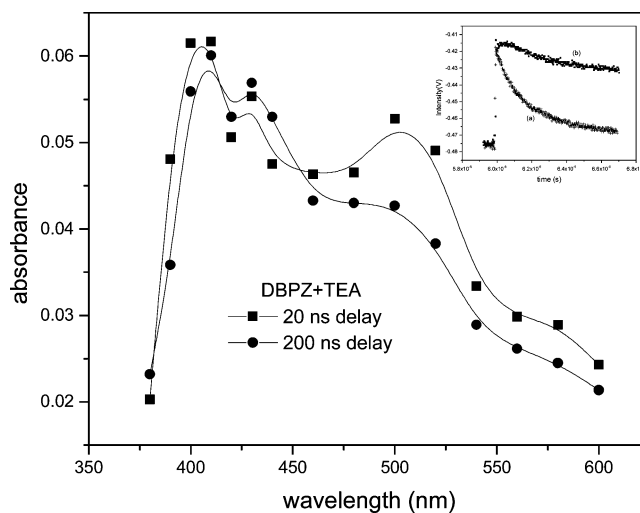


**Figure 5.** Transient absorption spectra of DBPZ ( $5 \times 10^{-5}$  M)–TEA ( $2.5 \times 10^{-3}$  M) in MeCN at a time delay 20 ns (■) and 200 ns (●) after the laser pulse. Inset shows the decay profile at 420 nm of (a) DBPZ ( $5 \times 10^{-5}$  M) (+) and (b) DBPZ ( $5 \times 10^{-5}$  M)–TEA ( $2.5 \times 10^{-3}$  M) (■) in MeCN.

This unusual behavior of TEA as compared to DMA/DMDPM may be attributed to the increasing oxidation potential of the bases as one goes from DMA to TEA ( $E_{1/2}$  vs SCE =  $0.76\text{V}$ <sup>33</sup> and  $0.96\text{V}$ <sup>34</sup> for DMA and TEA, respectively). The oxidation potential of DMDPM, however, is not available in the literature. But as DMDPM may be considered as two DMA molecules linked by a methylene group, it should have two nitrogen donor sites. So intuitively we can say that the  $E_{1/2}$  of DMDPM should be lower than that of DMA.<sup>35</sup> However, the higher oxidation potential of TEA than those of other aromatic amines is not the only reason behind its anomalous behavior as there are lots of examples in the literature where TEA is found to act as an electron donor.<sup>36</sup> The reason behind this observation, therefore, seems to be tied up with the size and structure of the donor and the acceptor molecules. The bulky aromatic bases DMA and DMDPM cannot come closer to the acceptor molecules, and the electron transfer occurs from a distance<sup>37</sup> in case of aromatic amines and the corresponding radical cations and anions are formed. For the DBPZ–DMDPM system, formation of RIP is favored rather by electron transfer than by excited-state complex formation (Figure 2). This might be due

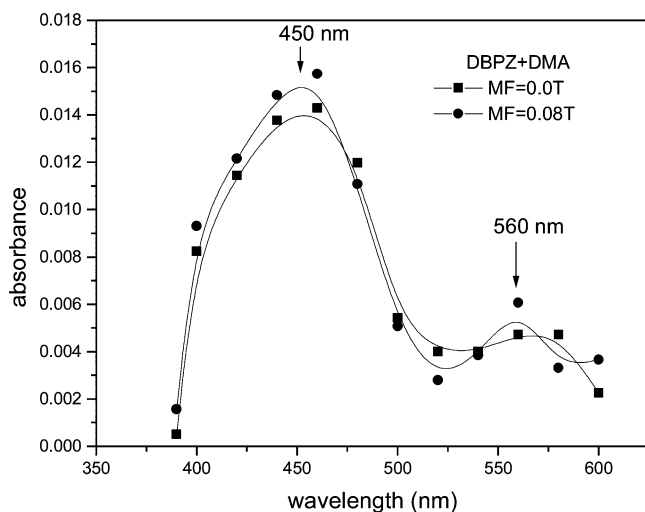


**Figure 6.** Transient absorption spectra of DBPZ ( $5 \times 10^{-5}$  M)–DMA ( $2.5 \times 10^{-3}$  M) in MeCN/0.1 M H<sub>2</sub>O mixture in absence (■) and presence (●) of 0.08 T MF at a delay of 0.6  $\mu$ s after the laser flash.

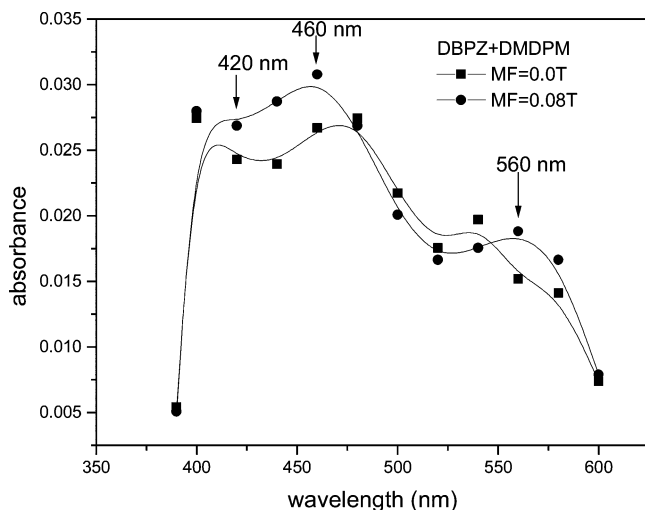


**Figure 7.** Transient absorption spectra of DBPZ ( $5 \times 10^{-5}$  M)–DMDPM ( $1.25 \times 10^{-3}$  M) in MeCN/0.1 M H<sub>2</sub>O mixture in absence (■) and presence (●) of 0.08 T MF at a delay of 0.6  $\mu$ s after the laser flash.

to the large size of DMDPM that hinders the donor and acceptor in coming close together. DMA, being a molecule of an intermediate size, encourages both electron transfer and excited-state complex formation at the same concentration as that of DMDPM (Figure 1), while TEA, being smaller in size, can very closely approach DBPZ. As a result it predominantly forms an excited-state charge-transfer complex. Interestingly, this charge-transfer complex is formed only with DBPZ but not with PZ. This might be due to the extended aromaticity of the DBPZ molecule that stabilizing the charge transfers complex. PZ lacking in this kind of stability cannot form such a complex.

**MFE in MeCN/H<sub>2</sub>O Mixture.** As mentioned earlier, most of the MFE studies on triplet originated radical pair dynamics using laser flash photolysis have been carried out in confined systems because the RIPs thereby remain geminate for a longer time than in a non-viscous medium. It is required for the successive processes of diffusion, spin evolution, and reencounter or free ion formation of the geminate RIPs to show appreciable MFE. From our previous discussion on MFE it is obvious that if the RIPs are initially formed in the singlet spin state, application of MF enhances such processes as would involve singlets, e.g., cage reaction or back electron transfer.

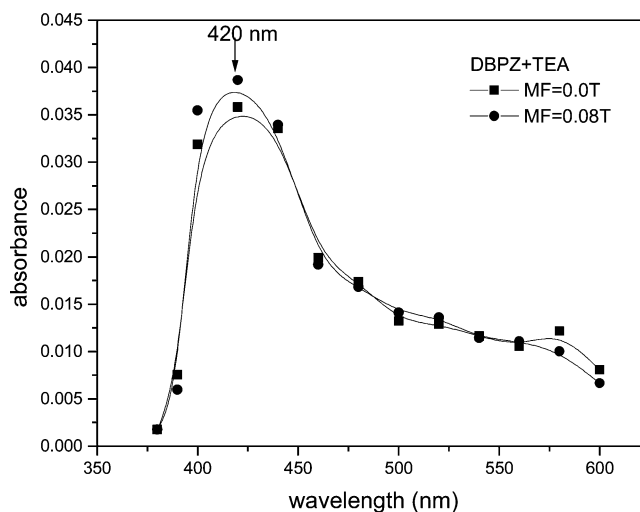


**Figure 8.** Transient absorption spectra of DBPZ ( $5 \times 10^{-5}$  M)–TEA ( $2.5 \times 10^{-3}$  M) in MeCN/0.1 M H<sub>2</sub>O mixture in absence (■) and presence (●) of 0.08 T MF at a delay of 0.6  $\mu$ s after the laser flash.

On the other hand, for the RIPs initially formed in the triplet state, MF enhances the triplet escape products. In the latter case, lifetime of the RIPs would increase or their decay constant would decrease in presence of an external MF. This phenomenon is reflected in the increase of the absorbance of the transients.

A prominent MFE is observed for all the DBPZ–amine systems. The absorbance values of both the charge-transfer species and radical ions are enhanced in the presence of an external MF (0.08 T), which indicates that all these transients have a triplet origin. On photoexcitation initially the <sup>1</sup>DBPZ\* is formed, which then undergoes a rapid ISC to form the <sup>3</sup>-DBPZ like PZ as reported earlier. The Scheme 1 describes mainly the interactions of the <sup>3</sup>DBPZ with amines. The equilibrium of the initial RIPs, formed due to electron transfer from amines to DBPZ, is further complicated by solvation equilibrium. Two types of RIPs might form: one is contact ion pair (CIP) or charge-transfer complex, and the other is solvent-separated ion pair (SSIP), which generates free ions on further solvation. The SSIP and charge-transfer complex behave differently in solvation and electronic coupling. The solvation is greater in the case of SSIP due to the intervening solvent molecules, whereas the electronic coupling is much more prominent in the charge-transfer species. It has been reported earlier that in polar solvent, electron transfer leads to the formation of SSIP prior to CIP.<sup>38</sup> Therefore, there is every possibility that triplet state charge-transfer complex (<sup>3</sup>ECT) and free ions form simultaneously from the initially formed triplet SSIPs (<sup>3</sup>SSIP). Now the <sup>3</sup>SSIP might be converted to <sup>1</sup>SSIP due to the presence of a small internal magnetic field, i.e., the hyperfine interaction (HFI) present in the system. When by diffusion the inter-radical distance becomes such that the exchange interactions between the two free electrons of the geminate RIP become negligible, maximum ISC occurs between the <sup>3</sup>SSIP and the <sup>1</sup>SSIP. Application of an external MF of the order of HFI suppresses the ISC by introducing Zeeman splitting in the triplet sublevels, which in turn increases the yield of the <sup>3</sup>SSIP as well as that of the <sup>3</sup>ECT and free ions. A peer investigation of MFE on different systems shows that the effect is quite prominent on both the free ions and the <sup>3</sup>ECT in DBPZ–DMA and DBPZ–DMDPM systems (Figures 6, 7), whereas in DBPZ–TEA system only the <sup>3</sup>ECT is affected by the MF (Figure 8). This dissimilar behavior might be due to the different size of the amines. Because of electron transfer from amines to DBPZ, the <sup>3</sup>SSIP is formed initially (path a). The formation of

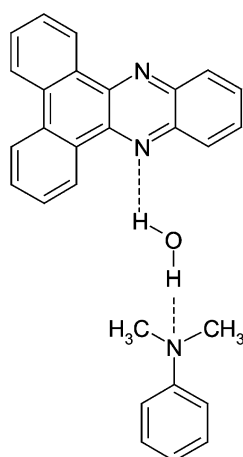
**TABLE 2: Variation of Triplet State Lifetime ( $\mu\text{s}$ ) of Different Acceptor–Donor Systems at 420 nm in MeCN/0.1 (M)  $\text{H}_2\text{O}$  Mixture with and without External Magnetic Field**

systems	without magnetic field	with magnetic field
DBPZ + DMA	0.338 ( $\pm 0.001$ )	0.341 ( $\pm 0.001$ )
DBPZ + DMDPM	0.829 ( $\pm 0.001$ )	0.836 ( $\pm 0.002$ )
DBPZ + TEA	1.831 ( $\pm 0.002$ )	2.437 ( $\pm 0.001$ )

**TABLE 3: Variation of Triplet State Lifetime ( $\mu\text{s}$ ) of Cation and Anion of DBPZ - DMDPM System at Respective Wavelengths in MeCN/0.1 (M)  $\text{H}_2\text{O}$  Mixture with and without External Magnetic Field**

species	without magnetic field	with magnetic field
DMDPM <sup>+a</sup>	0.707 ( $\pm 0.001$ )	1.260 ( $\pm 0.002$ )
DBPZ <sup>-b</sup>	0.737 ( $\pm 0.002$ )	0.858 ( $\pm 0.002$ )

<sup>a</sup> At 480 nm. <sup>b</sup> At 560 nm.

**CHART 2: The number of intervening water molecules might be more than one**

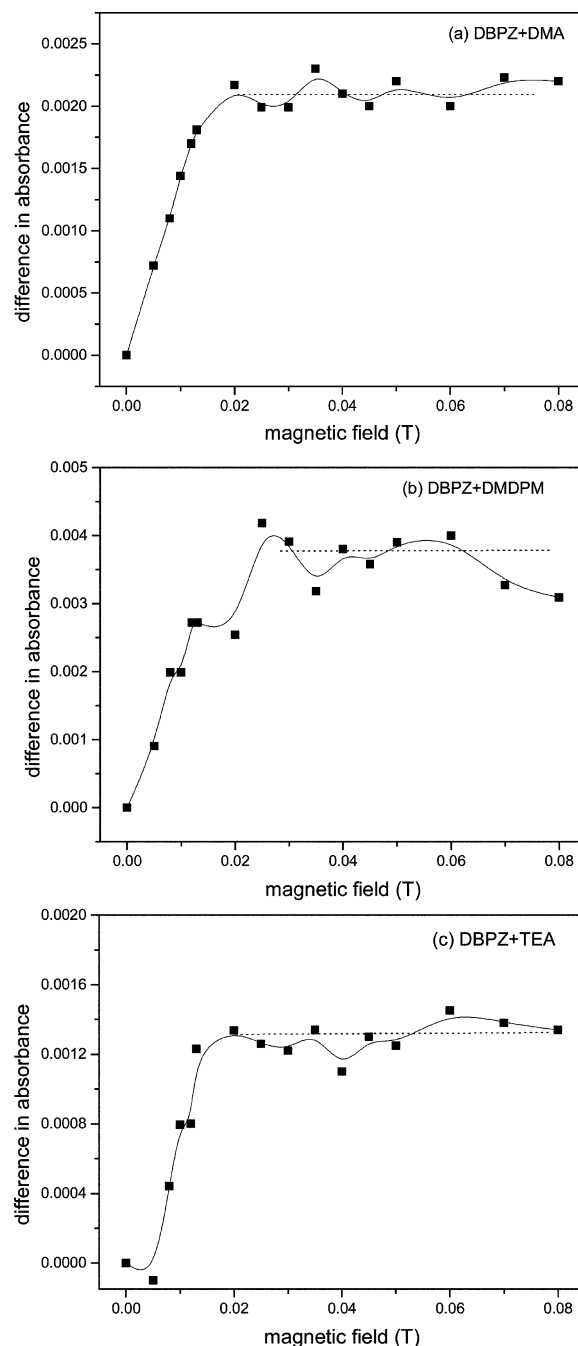
free ions from the <sup>3</sup>SSIP (path c) is favored for DMA/DMDPM because their approach toward the acceptor DBPZ molecules is hindered. On the other hand, closer vicinity of TEA and DBPZ facilitates the formation of the <sup>3</sup>ECT (path b). On application of an external MF, the equilibrium between <sup>3</sup>SSIP and <sup>1</sup>SSIP is perturbed, which is reflected in the enhancement of the lifetime of both the <sup>3</sup>ECT (Table 2) and free ions (Table 3).

Now, the question is this: why is MFE observed in this homogeneous MeCN/ $\text{H}_2\text{O}$  medium? In pure MeCN the effect is too small to be observed. Addition of a little of water (0.05–0.15 M) increases the MFE; i.e., it increases the stability of the geminate <sup>3</sup>SSIP with the right inter-radical distance where the exchange interaction is minimum and spin flipping can occur. It is possible only if the water molecules intervene the space between the DBPZ and amines. Therefore, the structure in Chart 2 with inter-radical hydrogen bonding, mediated by water might explain the observation. Due to hydrogen bonding (Supporting Information), the RIPs remain geminate, and inter-radical distance becomes such that the exchange interactions become negligible and spin evolution could be optimized. The variations of percentage magnetic field effect (%MFE) with the concentration of water for different DBPZ–amine systems are shown in Table 4. We have seen that the %MFE increases with an increase in water concentration and then decreases again. As mentioned earlier, the observation of MFE requires diffusion, spin flipping, and geminate recombination of the RIPs formed through PET. When the participating radical ions are very close to each other (at lower concentration of water), the exchange interaction will hinder spin conversion (singlet–triplet energy gap of SSIP is large). On the other hand, at higher water concentration, due to

**TABLE 4: Variation of Percentage Magnetic Field Effect with Concentration of Water Added<sup>a</sup>**

systems	water concentration (M)		
	0.05	0.10	0.15
DBPZ + DMA <sup>b</sup>	5.9%	9.5%	1.2%
DBPZ + DMDPM <sup>c</sup>	6.0%	15%	1.3%
DBPZ + TEA <sup>d</sup>	6.0%	8.4%	1.7%

<sup>a</sup> %MFE = [(OD (MF)–OD (MF=0))/OD (MF=0)]  $\times$  100. <sup>b</sup> At 450 nm. <sup>c</sup> At 460 nm. <sup>d</sup> At 420 nm.

**Figure 9.** The difference of absorbance with variation of MF for (a) DBPZ ( $5 \times 10^{-5}$  M)–DMA ( $2.5 \times 10^{-3}$  M) at 450 nm, (b) DBPZ ( $5 \times 10^{-5}$  M)–DMDPM ( $1.25 \times 10^{-3}$  M) at 460 nm, and (c) DBPZ ( $5 \times 10^{-5}$  M)–TEA ( $2.5 \times 10^{-3}$  M) at 420 nm in MeCN/0.1 M  $\text{H}_2\text{O}$  mixture at a delay of 0.6  $\mu\text{s}$  after the laser flash. The dotted lines depict saturation of the MFE.

large distance of separation between the radical ion pairs, the geminate characteristics of the SSIP and their spin correlation is lost and MFE decreases. For this reason MFE is maximized

**TABLE 5: Experimentally Obtained  $B_{1/2}$  Values of Different Acceptor–Donor Systems MeCN/0.1 (M) H<sub>2</sub>O Mixture**

system	$B_{1/2}$ (T)
DBPZ–DMA <sup>a</sup>	0.0081 (±0.0005)
DBPZ–DMDPM <sup>b</sup>	0.0089 (±0.0008)
DBPZ–TEA <sup>c</sup>	0.0098 (±0.0005)

<sup>a</sup> At 450 nm. <sup>b</sup> At 460 nm. <sup>c</sup> At 420 nm.

at an optimum water concentration. Here it is necessary to mention that more than one water molecule may intervene between the DBPZ and amine radical ions, to maintain the proper inter-radical distance where singlet–triplet energy gap of SSIP is negligible. We observe that the MFE is much more prominent on free ions (Table 3) than on <sup>3</sup>ECT (Table 2). This is because for DBPZ–DMA/DMDPM system the geminate triplet radical ions are well separated and are much more stabilized by hydrogen bonding. This inter-radical separation favors the spin evolution that is further affected by the external MF. TEA due to its closer approach to DBPZ reduces the optimum inter-radical distance in the geminate SSIP. Therefore, although the MFE is observed on <sup>3</sup>ECT, its magnitude is much less compared to the effect on the free ions in the two other systems (DBPZ–DMA and DBPZ–DMDPM).

Figure 9 shows the variation of “difference in absorbance” ( $\Delta OD$ ) with the MF where  $\Delta OD = OD(MF) - OD(MF = 0)$  is taken as a measure of the MFE. It is observed that  $\Delta OD$  increases with an increase in the MF strength and reaches saturation. The parameter  $B_{1/2}$  is defined as the MF required to attain half the saturation value for a particular system and is a measure of the HFI present in the system. The experimental  $B_{1/2}$  values for different DBPZ–amine systems are presented in Table 5. Our observations are consistent with the hyperfine coupling mechanism.

Theoretically  $B_{1/2}$  values can also be calculated from the hyperfine coupling constant ( $a_{iN}$ ) of individual radical ions as reported by Weller et al.<sup>39</sup> The  $a_{iN}$  values for DBPZ<sup>40</sup> and DMA<sup>41</sup> were obtained from the literature, and the calculated  $B_{1/2}$  value is 0.0049 T, which is slightly lower than the experimentally observed value. The  $a_{iN}$  values for the other amines were not available from the literature. However, DM-DPM can be considered as a dimmer of DMA and the calculated  $B_{1/2}$  is  $\sim 0.0010$  T, which is very close to the experimental value of  $B_{1/2}$ . On the contrary the  $B_{1/2}$  value for TEA appears to be much lower than the expected value since the calculated value for DBPZ–trimethylamine is only 0.0144 T.<sup>41</sup>

Deviation of the experimentally observed  $B_{1/2}$  values from those calculated could be explained in terms of the sizes of the different amine molecules. For the DBPZ–DMA system, the unpaired electron on the DMA radical cation can migrate to several diamagnetic DMA molecules in the vicinity before encountering the DBPZ radical anion.<sup>3,42–44</sup> Here the spin motion is perturbed not only by diffusion but also by hopping between donors of different nuclear configurations. The consequence of this hopping process is the increase the external MF strength required to overcome the HFI and enhance the width of the electron spin levels to effectively decouple the T<sub>+</sub>, T<sub>-</sub> states from S and T<sub>0</sub>. The hopping process manifests itself in a lifetime broadening and leads to an increase in the  $B_{1/2}$  value, which is reflected in the higher experimental  $B_{1/2}$  value than the calculated one. On the other hand, the bulky size of the DMDPM molecule hinders the approach of other DMDPM molecules toward DBPZ and the corresponding intermolecular electron hopping among the DMDPM molecules. Thus, HFI is the only operative mechanism, and the expected  $B_{1/2}$  value compares well with the experimental one.

In the case of DBPZ–TEA system the inter-radical distance in <sup>3</sup>ECT is such that the exchange interaction is not negligible; therefore the singlet and triplet states remain nondegenerate even at zero field. Thus the development of the actual spin flipping is somehow lessened by the very fast inter-radical electron exchange. So the experimentally obtained  $B_{1/2}$  value is lower than that calculated. Schulten predicted earlier that for a sterically fixed intramolecular system the HFI constant could assume half the values compared to the intermolecular one and Petrov et al. did indeed verify experimentally the effect of this exchange narrowing on  $B_{1/2}$ .<sup>45,46</sup>

## Conclusions

From this work we infer that the structure of a molecule can control its photophysical characteristics. The behavior of PZ is changed when two benzene rings are attached to it. The steric bulk of the DBPZ molecule helps in the formation of <sup>3</sup>ECT as well as in showing MFE in homogeneous MeCN/H<sub>2</sub>O mixture. The observed MFE could be explained by considering inter-radical hydrogen bonding via the intervening water molecules, which helps to sustain the geminate characteristics and hence the spin correlation in the RIPs. Moreover, the experimentally observed  $B_{1/2}$  values for different DBPZ–amine systems also support that HFI plays a crucial role in all the systems, although it is reduced to some extent in the <sup>3</sup>ECT of the DBPZ–TEA system by fast electron exchange in the geminate RIPs.

**Acknowledgment.** We sincerely thank Mrs. Chitra Raha of SINP for her kind assistance and technical support. We thank Prof. Atri Mukhopadhyay of SINP for his kind help in revising the manuscript. We also thank Ms. Kakali Sen of IISC, Bangalore, Ms. Sharmistha Dutta Choudhury of SINP, Ms. Ajanta Mukherjee and Ms. Sulakshana Karmakar of Bose Institute and Ms. Doyel Das of IACS, India for their cooperation.

**Supporting Information Available:** Fluorescence spectrum. This material is available free of charge via the Internet at <http://pubs.acs.org>.

## References and Notes

- Balzani, V., Ed. In *Electron Transfer in Chemistry*; Wiley-VCH Verlag GmbH: Weinheim, Germany, 2001; Vols. 1–5.
- Steiner, U. E.; Ulrich, T. *Chem. Rev.* **1989**, *89*, 51 and references therein.
- Bhattacharya, K.; Chowdhury, M. *Chem. Rev.* **1993**, *93*, 507.
- In *Dynamic Spin Chemistry Magnetic Controls and Spin Dynamics of Chemical Reactions*; Nagakura, S., Hayashi, H., Azumi, T. Eds.; Kodansha Ltd.: Tokyo, 1998.
- Gould, I. R.; Turro, N. J.; Zimmt, M. B. *Adv. Phys. Org. Chem.* **1984**, *20*, 1.
- Tanimoto, Y.; Fujiwara, Y. In *Handbook of Photochemistry and Photobiology: Inorganic Chemistry*; Nalwa, H. S., Ed.; American Scientific Publishers: Stevenson Ranch, CA, 2003; Vol. 1.
- Grissom, C. B. *Chem. Rev.* **1995**, *95*, 3.
- Boxer, S. G.; Chidsey, C. E. D.; Roelofs, M. G. *Ann. Rev. Phys. Chem.* **1983**, *34*, 389.
- Dutta Choudhury, S.; Basu, S. *J. Phys. Chem. A* **2005**, *109*, 8113.
- Sengupta, T.; Choudhury, S. D.; Basu, S. *J. Am. Chem. Soc.* **2004**, *126*, 10589.
- Brana, M. F.; Cacho, M.; Gradillas, A.; de Pascual-Teresa, B.; Ramos, A. *Curr. Pharm. Des.* **2001**, *7*, 1745.
- Turro, N. J.; Weed, G. C. *J. Am. Chem. Soc.* **1983**, *105*, 1861.
- Scaiano, J. C.; Joanovic, S. V.; Morris, D. G. *J. Photochem. Photobiol. A* **1998**, *113*, 197.
- Periasamy, N.; Linschitz, H. *Chem. Phys. Lett.* **1979**, *64*, 281.
- Shafirovich, V. Y.; Batova, E. E.; Levin, P. P. *J. Phys. Chem. A* **1993**, *97*, 4877.
- Steiner, U. E.; Haas, W. *J. Phys. Chem.* **1991**, *95*, 1880.
- Mori, Y.; Sakaguchi, Y.; Hayashi, H. *J. Phys. Chem. A* **2002**, *106*, 4453.

- (18) Mori, Y.; Sakaguchi, Y.; Hayashi, H. *J. Phys. Chem. A* **2000**, *104*, 4896.
- (19) Igarashi, M.; Sakaguchi, Y.; Hayashi, H. *Chem. Phys. Lett.* **1995**, *243*, 545.
- (20) Aich, S.; Basu, S. *Chem. Phys. Lett.* **1997**, *281*, 247.
- (21) Sakaguchi, Y.; Hayashi, H. *J. Phys. Chem. A* **1997**, *101*, 549.
- (22) Ali, S. S.; Maeda, K.; Murai, H.; Azumi, T. *Chem. Phys. Lett.* **1997**, *267*, 520.
- (23) Levin, P. P.; Raghavan, P. K. N.; Kuzmin, V. A. *Chem. Phys. Lett.* **1990**, *167*, 67.
- (24) Shimada, E.; Nagano, M.; Iwahashi, M.; Mori, Y.; Sakaguchi, Y.; Hayashi, H. *J. Phys. Chem. A* **2001**, *105*, 2997.
- (25) Steiner, U. *Chem. Phys. Lett.* **1980**, *74*, 108.
- (26) Mori, Y.; Sakaguchi, Y.; Hayashi, H. *Chem. Phys. Lett.* **1998**, *286*, 446.
- (27) Ulrich, T.; Steiner, U. E.; Foell, R. E. *J. Phys. Chem.* **1983**, *87*, 1873.
- (28) Amashukeli, X.; Winkler, J. R.; Gray, H. B.; Gruhn, N. E.; Lichtenberger, D. L. *J. Phys. Chem. A* **2002**, *106*, 7593.
- (29) Aich, S.; Basu, S. *J. Chem. Soc. Faraday Trans.* **1995**, *91*, 1593.
- (30) Shida, T.; Hamill, W. H. *J. Chem. Phys.* **1966**, *44*, 2369.
- (31) Dutta Choudhury, S.; Basu, S. *Chem. Phys. Lett.* **2004**, *383*, 533.
- (32) Ogata, T.; Yamamoto, Y.; Wada, Y.; Murakoshi, K.; Kusaba, M.; Nakashima, N.; Ishida, A.; Takamuku, S.; Yanagida, S. *J. Phys. Chem.* **1995**, *99*, 11916.
- (33) Nad, S.; Pal, H. *J. Phys. Chem. A* **2000**, *104*, 673.
- (34) Buntinx, G.; Valat, P.; Wintgens, V.; Poizat, O. *J. Phys. Chem.* **1991**, *95*, 9347.
- (35) Dutta Choudhury, S.; Basu, S. *Chem. Phys. Lett.* **2003**, *373*, 67.
- (36) Ghosh, H. N.; Pal, H.; Sapre, A. V.; Mittal, J. P. *J. Am. Chem. Soc.* **1993**, *115*, 11722.
- (37) Bolton, J. R.; Mataga, N.; McLendon, G. *Electron Transfer in Inorganic, Organic and Biological Systems*; Advanced Chemistry Series 228; American Chemical Society: Washington, DC, 1991.
- (38) Crawford, M. K.; Wang, Y.; Eisenthal, K. B. *Chem. Phys. Lett.* **1981**, *79*, 529.
- (39) Staerk, H.; Treichel, R.; Weller, A. *Chem. Phys. Lett.* **1983**, *96*, 28.
- (40) Sevenster, A. J. L.; Tabner, B. J. *Org. Mag. Reson.* **1984**, *22*, 521.
- (41) *Landolt-Bornstein-Group II Molecules and Radicals*; Springer-Verlag: Heidelberg, Germany, 1992.
- (42) Kruger, H. W.; Michael-Beyerle, M. E.; Seidlitz, H. *Chem. Phys. Lett.* **1982**, *87*, 79.
- (43) Sen, K.; Bandyopadhyay, S.; Bhattacharya, D.; Basu, S. *J. Phys. Chem. A* **2001**, *105*, 9077.
- (44) Grampp, G.; Justinek, M.; Landgraf, S. *Mol. Phys.* **2002**, *100*, 1063.
- (45) Schulten, K. *J. Chem. Phys.* **1985**, *82*, 1312.
- (46) Petrov, N. Kh.; Alfimov, M. V.; Budyka, M. F.; Gavrishova, T. N.; Staerk, H. *J. Phys. Chem. A* **1999**, *103*, 9601.